

## **Effect of Corrosion Inhibitor Head Group on the Electrochemical Processes Governing CO<sub>2</sub> Corrosion**

J.M. Domínguez Olivo <sup>a</sup>, Shuyun Cao <sup>a,b</sup>, D. Young <sup>a</sup>, B. Brown <sup>a</sup>, S. Netic <sup>a</sup>

<sup>a</sup>Institute for Corrosion and Multiphase Technology, Department of Chemical & Biomolecular Engineering, Ohio University, Athens, OH 45701

<sup>b</sup>State Key Laboratory of Separation Membranes and Membrane Processes & School of Material Science and Engineering, Tianjin Polytechnic University, Tianjin, 300387, P.R. China

### **ABSTRACT**

The use of corrosion inhibitors is a common practice used to mitigate internal pipeline corrosion in the oil and gas industry. An organic corrosion inhibitor is a molecule comprised of a head group (hydrophilic part) and an alkyl tail (hydrophobic part). Despite the significant amount of work associating the effect of the head group with the mode of adsorption of the inhibitor (such as bonding, effect on the tilt angle of the tail, and hysteresis), there is a lack of research relating the effect of the head group with the electrochemical processes governing the corrosion of mild steel in CO<sub>2</sub> saturated environments. In order to isolate the effect of the head group on the electrochemical processes underlying corrosion, three different model compounds with the same alkyl tail length (10 carbon atoms) and different head groups were synthesized in-house. The head groups included a Brønsted acid ionic liquid (imidazole-sulfonic acid-type), a zwitterion (imidazole-type) and a quaternary ammonium-type. By performing experiments at pH 4, 30 °C, using an X65 steel rotating cylinder electrode at 1000 RPM, corrosion rate and potentiodynamic polarization curves showed that the head group has a significant impact on the corrosion mechanisms associated with CO<sub>2</sub> corrosion. This was particularly true when it comes to the activation energy of the charge transfer reactions governing the CO<sub>2</sub> corrosion process. Finally, an electrochemical model (based on a modified Butler-Volmer equation) was developed based on the changes in activation energy produced by each corrosion inhibitor.

## INTRODUCTION

A corrosion inhibitor is a chemical substance that, added in small concentrations (in the order of part per million), can diminish corrosion in certain environments.<sup>1</sup> Among all types of corrosion inhibitors, organic-type corrosion inhibitors are widely used in the control of internal pipeline corrosion in the oil and gas industry.<sup>2,3</sup> Organic corrosion inhibitors are typically surfactant-type corrosion inhibitors with a hydrophilic head group and a hydrophobic alkyl tail.<sup>2,4</sup>

The most commonly accepted model of corrosion inhibition by this type of corrosion inhibitor is the blockage model, as presented for example in the book edited by McCafferty, *et al.*<sup>2</sup> This approach states that the anodic dissolution of a metal is “blocked” by the head group of the corrosion inhibitor (which is “bonded” with the metal surface), while the tail of the inhibitor molecule “confers additional protection” by blocking reducible species affecting the cathodic reaction.<sup>2</sup> Therefore, in this approach, it appears that the head group would be the governing factor in the inhibition process, retarding mostly the anodic dissolution by blockage. However, other researchers have found that, given the same head group, an increase in the tail length would also decrease the anodic dissolution.<sup>4,5</sup> Zhu, *et al.*, in a recent review<sup>6</sup> indicated that the role of the tail may influence the formation of micelles, that produce a better coverage of the surface.<sup>6</sup>

However, Dominguez, *et al.*,<sup>5</sup> worked with inhibitors with the same head group and different tail lengths. The concentrations were below the critical micelle concentration and the tendency of a higher efficiency was still governed by the alkyl tail length.<sup>5</sup> Additionally, the authors described the inhibition process in a more mechanistic way.<sup>5</sup> In the inhibition process, it should be understood that the adsorption of the corrosion inhibitors would not simply “block” the electrochemical reactions. Instead, the charge transfer rates would be diminished due to the dilution of water at the metal interface caused by the displacement and replacement of water molecules from the metal surface<sup>5</sup>. Such a condition increases the activation energy of the charge transfer processes, “retarding” the rate of the electrochemical reactions rather than just “blocking” them.<sup>5</sup> Such a postulate was tested in the past with the use of four corrosion inhibitor model compounds with the same head group (quaternary ammonium) and different tail lengths (butyl, octyl, dodecyl and hexadecyl)<sup>5</sup>. It was proven that the adsorption of such inhibitors changed the activation energy of the electrochemical reactions associated with CO<sub>2</sub> corrosion of mild steel.

In a research article from 2016<sup>7</sup> it was concluded that, given the same conditions of flow, pH and temperature, the addition of a corrosion inhibitor increased the activation energy of the electrochemical process underlying CO<sub>2</sub> corrosion as depicted in Figure 1.

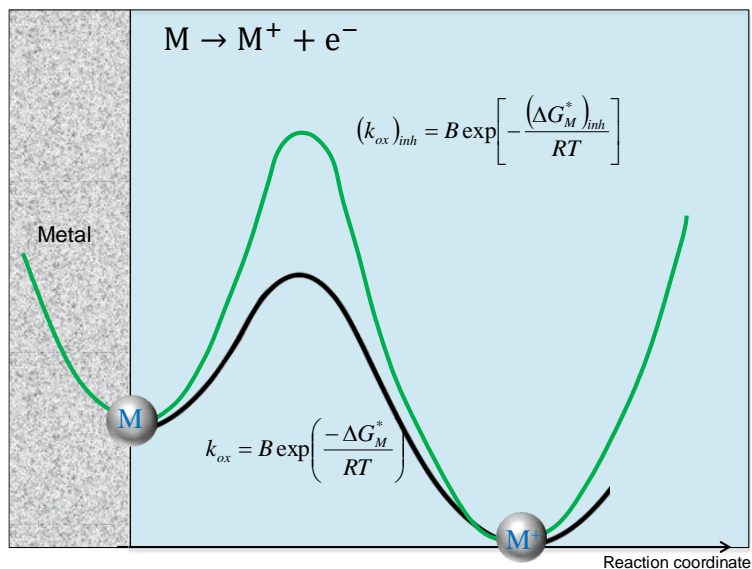


**Figure 1. Effect of the addition of corrosion inhibitor in the activation energy of the electrochemical process of corrosion: the activation energy of the process with no corrosion inhibitor ( $\Delta G_M$ ) increases to  $(\Delta G_M)_{inh}$  when a corrosion inhibitor adsorbs onto the metal surface**

Such an increase in the activation energy was correlated to the alkyl tail length of the corrosion inhibitor model compounds which had been tested, as Figure 2 shows.

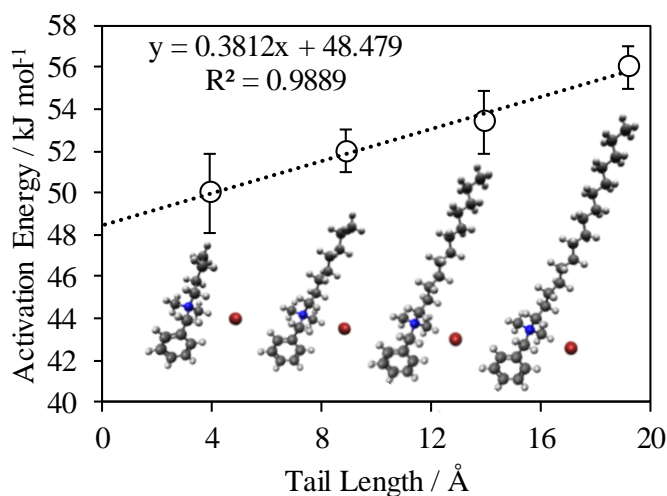


**Figure 2. Increase of activation energy of the electrochemical process governing CO<sub>2</sub> corrosion with respect to the alkyl tail length of quaternary ammonium bromide inhibitors<sup>7</sup>.**

From extrapolation, Figure 2 shows that a “zero tail length” inhibitor would result in an activation energy similar to having a similar environment with no inhibitor present (ca. 48

$\text{kJ mol}^{-1}$ ).<sup>7</sup> Such a result implies that the alkyl tail length is the dominating factor in the inhibition process. It can be hypothesized that the head group does not play a significant role in the corrosion mitigation process. However, before accepting this generalized conclusion, the present research work was focused on investigating the effect of the head group on corrosion mitigation in the same environmental conditions.

## METHODOLOGY

### Synthesis of Corrosion Inhibitor Model Compounds

Three different model compounds were synthesized in house and tested. Three model compounds consisted of the same tail length, decyl ( $-\text{C}_{10}\text{H}_{21}$ ), with different head groups of imidazole-sulfonic acid, imidazole, and quaternary ammonium. The synthesis of the quaternary ammonium compound is described elsewhere<sup>7</sup>. Regarding the imidazole-type of compounds, the synthesis was performed based on previous research.<sup>8-11</sup> The general procedure is depicted in Figure 3.

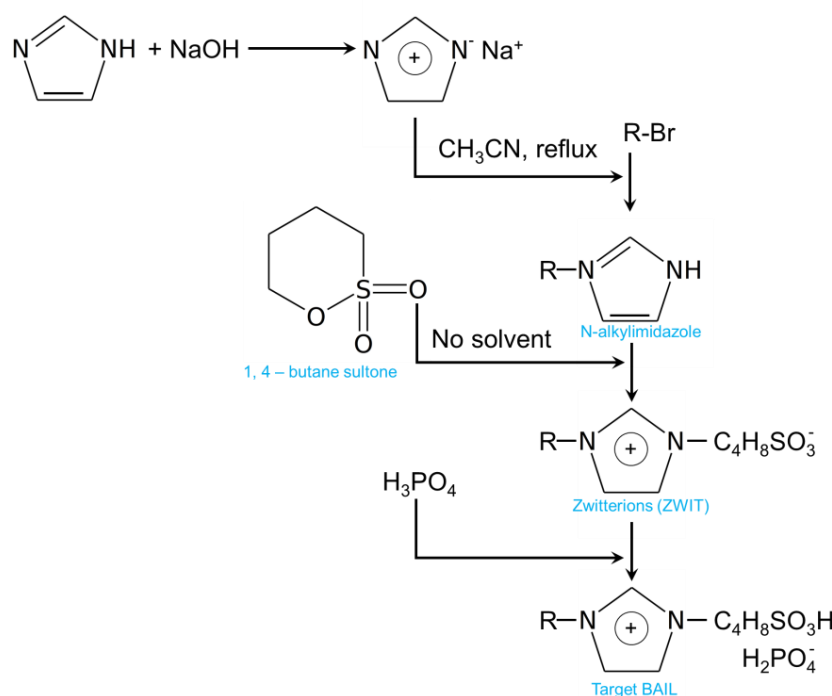


**Figure 3. General synthetic route for the imidazole and imidazole-sulfonic acid-type of corrosion inhibitor model compounds.**

**Table 1**  
**Molecular structure of the corrosion inhibitor model compounds**

Inhibitor Structure	Inhibitor Name
	BAIL-C10 (imidazole-sulfonic acid-type)
	ZWIT-C10 (imidazole-type)
	Q-C10 (quaternary ammonium-type)

### Electrochemical Techniques

A three-electrode glass cell set up was used to perform corrosion and corrosion mitigation experiments at 1 bar, pH 4 at 30 °C. In a 1 wt % NaCl solution, an API 5L X65 steel rotating cylinder electrode (RCE) at 1000 rpm was used as the working electrode as shown in Figure 4.

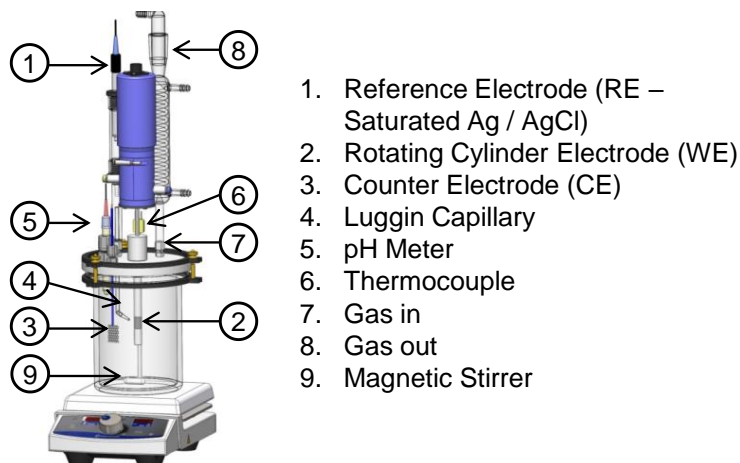


**Figure 4: Three-electrode set up used to perform experiments.<sup>1</sup>**

<sup>1</sup> Image courtesy of Cody Shafer, ICMT, Ohio University.

The composition of the steel is shown in Table 2. A platinum covered titanium mesh was used as a counter electrode and a saturated Ag/AgCl<sub>sat</sub> reference electrode was used as the reference. CO<sub>2</sub> was used for purging the system and the solution pH was adjusted and maintained at pH 4.0±0.1 during each experiment.

**Table 2**  
**Chemical Composition of the X65 Steel Used as Working Electrode**

Composition	Elements									
	Cr	Mo	S	V	Si	C	Ni	Mn	P	Fe
Weight %	0.14	0.16	0.009	0.047	0.26	0.13	0.36	1.16	0.009	Balance

The working concentrations of each inhibitor were the minimum concentration that yielded the maximum efficiency. Those concentrations were obtained with a methodology previously described<sup>7</sup>. The molecular structure of the corrosion inhibitor model compounds is given in Table 1. Linear polarization resistance (LPR) measurements were used to obtain the charge transfer resistance by polarizing the working electrode from -5 mV to +5 mV with respect to the corrosion potential at a scan rate of 0.125 mV/s; corrosion rates were then calculated by using a *B* value of 26 mV/decade. Electrochemical impedance spectroscopy (EIS) measurements were used for measuring solution resistance by using an oscillating potential of ±15 mV (*V*<sub>rms</sub> = 10 mV) with respect to the corrosion potential. A summary of tested conditions is given in Table 3.

**Table 3**  
**Summary of Experimental Conditions**

Description	Parameters
Working solution	1 wt% NaCl
Sparge gas	CO <sub>2</sub>
Temperature / °C	30
pH	4.0 ± 0.1
Corrosion inhibitors model compound concentration	Q-C10 (quat-type) (200 ppm <sub>v</sub> ) BAIL-C10 (imidazole-sulfonic acid-type) (80 ppm <sub>v</sub> ) ZWIT-C10 (imidazole-type) (80 ppm <sub>v</sub> )
Measurement methods	LPR, EIS

## RESULTS AND DISCUSSION

### Corrosion Rate Experiments (LPR)

Figure 5 shows the corrosion rate with time for the model compounds at their respective surface saturation concentration. It can be observed that the corrosion inhibitor ZWIT-C10 exhibited a higher efficiency at steady state than its counterparts Q-C10 and BAIL-C10 by a factor of two.

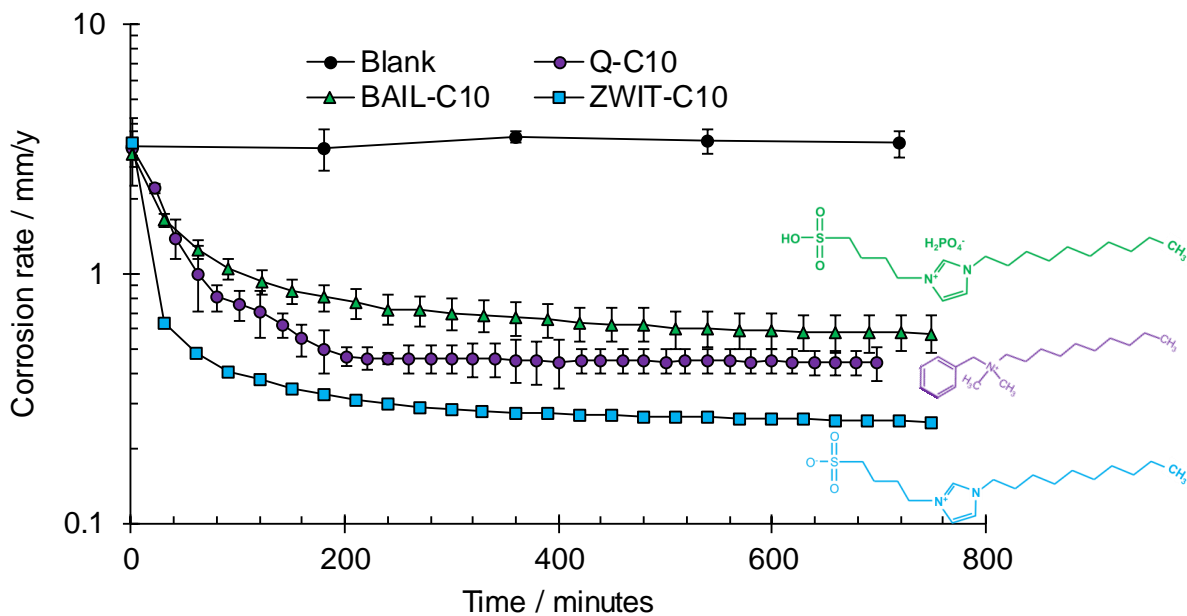


**Figure 5. Corrosion rate with time with time for different corrosion inhibitor model compounds. Each corrosion inhibitor model compound tested at the surface saturation concentration.**

### Corrosion Mechanisms

Corrosion mechanisms were studied and compared by performing potentiodynamic polarizations after the steady-state was reached with respect to the LPR corrosion rate. Figure 6 shows the potentiodynamic curves. It can be observed that the limiting currents were not affected by the presence of any of the model compounds. This result suggests that the active surface area of the steel surface was not diminished significantly (as the “blockage” model would imply). Such an observation is in good agreement with the central postulate of this whole research<sup>5</sup>: the inhibition was not caused mainly by the blockage effect by the head group as suggested by McCafferty *et al*<sup>2</sup>.

On the other hand, it was also observed that although the corrosion inhibitors possess the same alkyl tail length, the cathodic and anodic charge transfer mechanisms were retarded to a different extent. This result suggests that the retardation of the electrochemical reactions was not only caused by the alkyl tail, the head group also played a role in the retardation of charge transfer reactions.

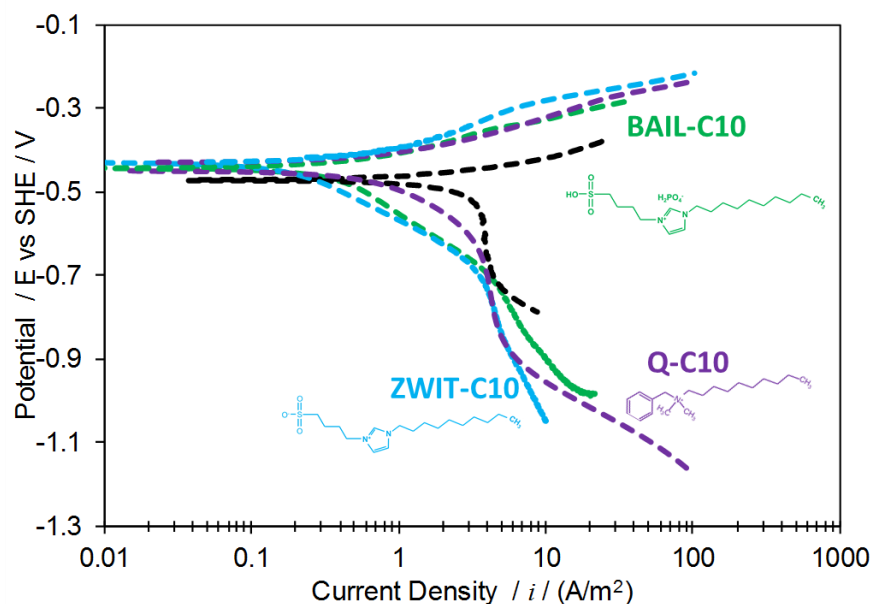


**Figure 6. Measured potentiodynamic polarization curves for corrosion inhibitor model compounds**

### Activation Energy of Charge Transfer Processes

The effect of the corrosion inhibitor model compounds on the charge transfer reactions was also studied by calculating the activation energy of the charge transfer rates as described elsewhere<sup>5</sup>. Figure 7 shows the comparison of such activation energies. It was observed that different compounds changed the activation energy.

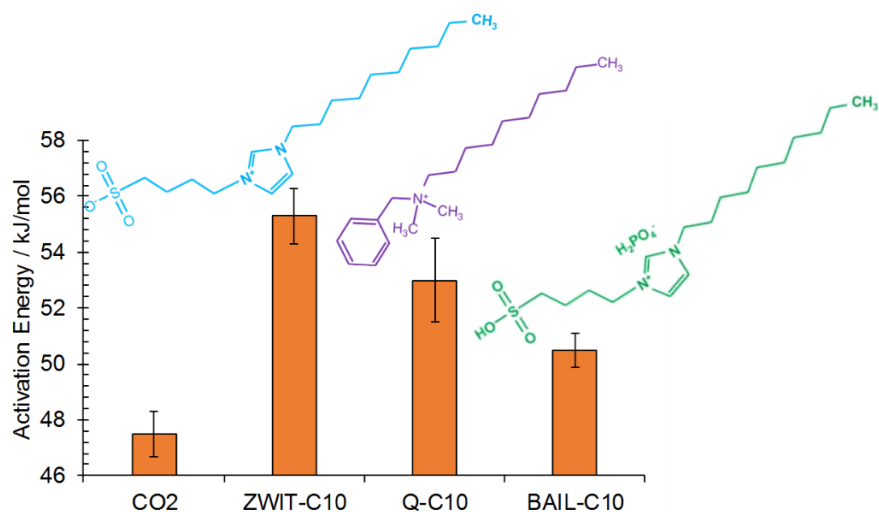


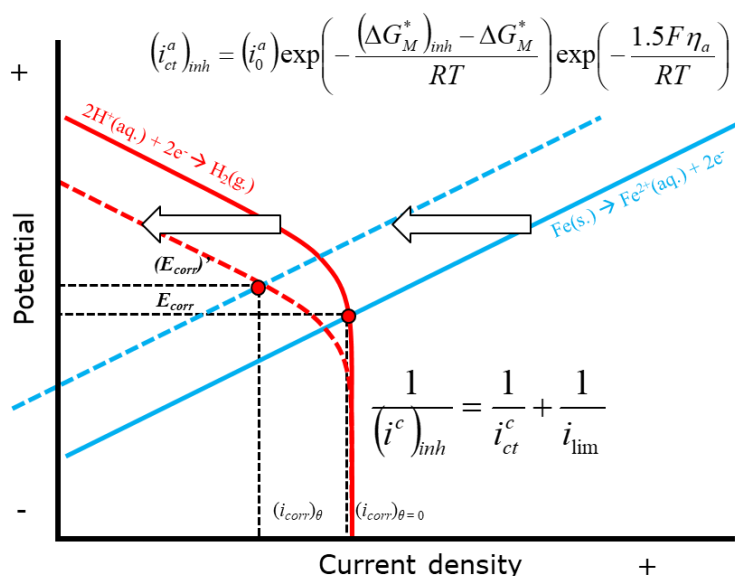
**Figure 7. Activation energies for charge transfer reactions with and without corrosion inhibitors.**



These experimental observations lead to the rejection of the initial hypothesis: the alkyl tail length is not the only factor to consider. We can state the corrosion inhibitor head group does play a role in the retardation of the charge transfer reactions in CO<sub>2</sub> corrosion.

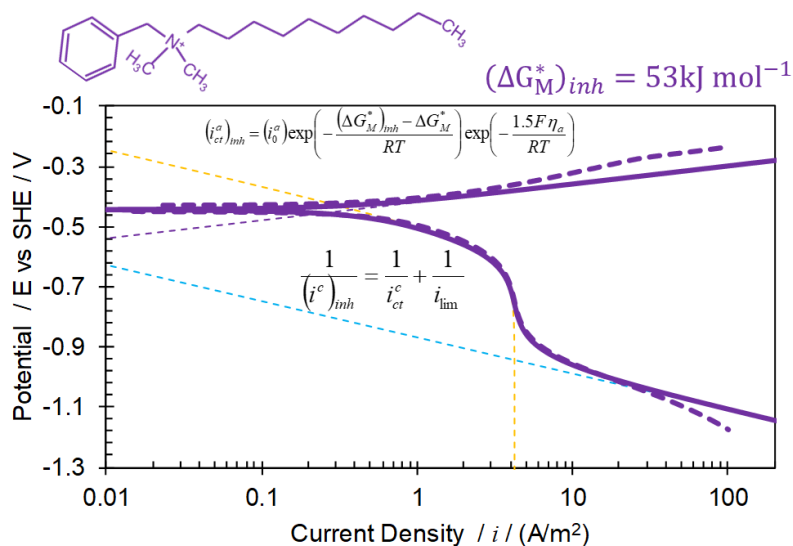
### Activation Energy of Charge Transfer Processes

After determining the activation energies for charge transfer reactions, the corrosion mechanisms were modeled with an electrochemical model described in previous research<sup>5</sup> and shown again in Figure 8. The electrochemical model is based on the increase in the activation energy and subsequent retardation of charge transfer reaction rates while limiting currents remain unaffected. As a result, the corrosion rate decreases and the corrosion potential increases. Values of activation energies from Figure 7 were used in the model equations.



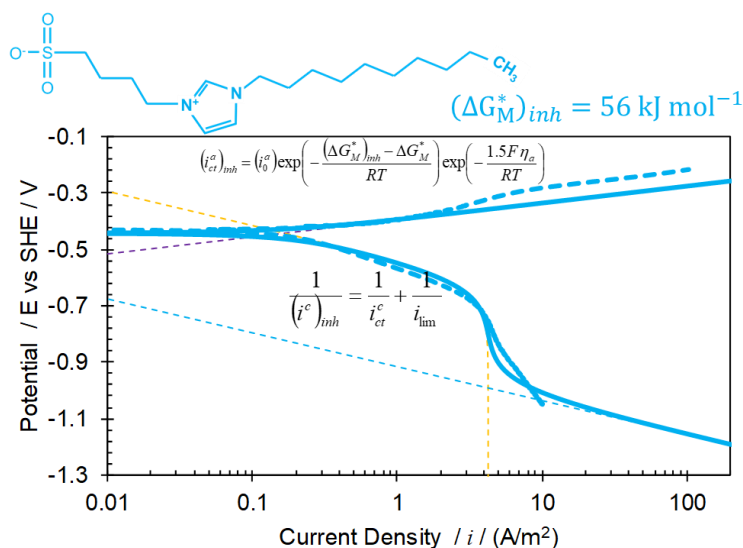
**Figure 8. Basic principles of the electrochemical model for CO<sub>2</sub> corrosion in the presence of corrosion inhibitors. Model Equations:  $\Delta G_M$  is the activation energy with no inhibitor (47.5 kJ mol<sup>-1</sup>);  $(\Delta G_M)_{inh}$  is the activation energy in the presence of an inhibitor.**

Figure 9 shows the predicted potentiodynamic sweep for CO<sub>2</sub> corrosion mechanisms in the presence of the corrosion inhibitor model compound Q-C10 as a solid line and the experimental data as the dotted line. The model is in good agreement with the experimental potentiodynamic polarization sweep.



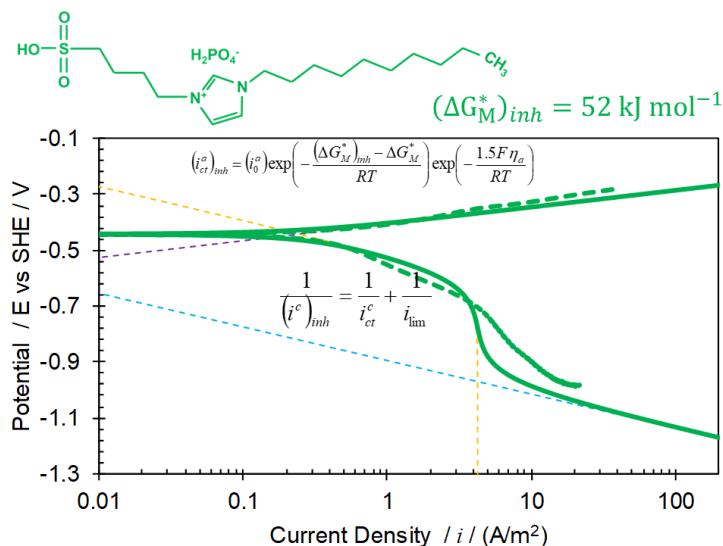
**Figure 9. Predicted (solid line) and measured (dotted line) potentiodynamic polarization curves for corrosion inhibitor model compound Q-C10.**

Figure 10 shows the predicted and measured potentiodynamic sweeps for the corrosion inhibitor model compound IL-S-C10. There is a good agreement between the model and the experimental potentiodynamic sweep.



**Figure 10. Predicted (solid line) and measured (dotted line) potentiodynamic polarization curves for corrosion inhibitor model compound IL-S-C10.**

Again, Figure 11 shows an acceptable match between the electrochemical model and the experimental sweeps for the corrosion inhibitor IL-C10.



**Figure 11. Predicted (solid line) and measured (dotted line) potentiodynamic polarization curves for corrosion inhibitor model compound IL-C10.**

All the curves and the activation energies are in good agreement with the electrochemical model proposed. Thereby, the effect of a corrosion inhibitor can be quantified by changes in the activation energy of charge transfer processes. This finding also implies that there is no preferential blockage by the corrosion inhibitor<sup>5</sup>. In other words, both anodic and cathodic charge transfer reactions were retarded to the same extent.

## CONCLUSIONS

- Different secondary groups attached to the main head can also play a significant role. In this case, the presence of sulfonic acid in an imidazole head group modified the inhibition properties of the inhibitor as compared to the sole imidazole head group.
- The proposed model of corrosion inhibition based on the change in the activation energy of the electrochemical reaction satisfactorily described the inhibition process. Both anodic and cathodic reactions were retarded to the same extent, suggesting that there was no preferential blocking any of the inhibitor head groups tested.

## ACKNOWLEDGMENTS

The author would like to thank the following companies for their financial support:

Anadarko, Baker Hughes, BP, Chevron, CNOOC, ConocoPhillips, DNV GL, ExxonMobil, M-I SWACO (Schlumberger), Multi-Chem (Halliburton), Occidental Oil Company, Pioneer Natural Resources, Saudi Aramco, Shell Global Solutions, SINOPEC (China Petroleum), and TOTAL.

## REFERENCES

1. V. S. Sastri, *Green Corrosion Inhibitors*, 2<sup>nd</sup> ed. (Hoboken, NJ: John Wiley & Sons, 2011), p. 110.
2. E. McCafferty, *Introduction to corrosion science*, (New York, NY: Springer, 2010), pp. 359-400.
3. D. A. Jones, *Principles and prevention of corrosion*, 2<sup>nd</sup> ed. (New York, NY: MacMillan, 1996), pp. 503-570.
4. A. Edwards, C. Osborne, S. Webster, D. Klenerman, M. Joseph, P. Ostovar, and M. Doyle, "Mechanistic studies of the corrosion inhibitor oleic imidazoline," *Corrosion Science* 36, 2, (1994): pp. 315–325
5. J.M. Dominguez Olivo, D. Young, B. Brown, S. Nescic, "Effect of corrosion inhibitor alkyl tail length on the electrochemical process underlying CO<sub>2</sub> corrosion of mild steel," NACE Corrosion Conference 2018, paper 11537 (Houston, TX: NACE, 2018).
6. Y. Zhu, M. Free, R. Woollam, W. Durnie, "A review of surfactants as corrosion inhibitors and associated modeling," *Prog. Mater. Sci.* 90, (2017): pp. 159-223.
7. J. M. Dominguez Olivo, B. Brown, and S. Nescic, "Modeling of corrosion mechanisms in the presence of quaternary ammonium chloride and imidazoline corrosion inhibitors," NACE Corrosion Conference 2016, paper 7406 (Houston, TX: NACE, 2016).
8. A. C. Cole, J. Jensen, I. Ntai, K. L. T Tran, K. J. Weaver, D. C. Forbes, J. H. Davis, "Novel brønsted acidic ionic liquids and their use as dual solvent-catalysts," *J. Am. Chem. Soc.*, 124, 21 (2002): pp. 1-16.
9. J. Gui, X. Cong, D. Liu, X. Zhang, Z. Hu, Z. Sun, "Novel brønsted acidic ionic liquid as efficient and reusable catalyst system for esterification," *Catal. commun.*, 5 (2004): pp. 473-477.
10. P. Bonhote, A. Dias, N. Papageorgiou, K. Kalyanasundaram, and M. Gratzel, "Hydrophobic, highly conductive ambient-temperature molten salts," *Inorg. Chem.*, 33 (1995): pp. 1168-1178.
11. S. Duan, X. Jing, D. Li, and H. Jing, "Catalytic asymmetric cycloaddition of CO<sub>2</sub> to epoxides via chiral bifunctional ionic liquids," *J. Mol. Cat. A: Chem.*, 411 (2016): pp. 35-39